Detecting quantum non-breaking channels without entanglement

Huan-Yu Ku,[1,2,*] Josef Kadlec,[3] Antonín Černoch,[4] Marco Túlio Quintino,[5,6] Wenbin Zhou,[7] Karel Lemr,[3] Neill Lambert,[2] Adam Miranowicz,[8,2] Shin-Liang Chen,[1,9,†] Franco Nori,[2,10,11] and Yueh-Nan Chen[1,2,‡]

[1] *Department of Physics and Center for Quantum Frontiers of Research & Technology (QFort), National Cheng Kung University, Tainan 701, Taiwan*
[2] *Theoretical Quantum Physics Laboratory, RIKEN Cluster for Pioneering Research, Wako-shi, Saitama 351-0198, Japan*
[3] *RCPTM, Joint Laboratory of Optics of Palacký University and Institute of Physics of Czech Academy of Sciences, 17. listopadu 12, 771 46 Olomouc, Czech Republic*
[4] *Institute of Physics of the Czech Academy of Sciences, Joint Laboratory of Optics of PU and IP AS CR, 17. listopadu 50A, 772 07 Olomouc, Czech Republic*
[5] *Vienna Center for Quantum Science and Technology (VCQ), Faculty of Physics, University of Vienna, Boltzmanngasse 5, 1090, Vienna, Austria*
[6] *Institute for Quantum Optics and Quantum Information (IQOQI), Austrian Academy of Sciences, Boltzmanngasse 3, A-1090 Vienna, Austria*
[7] *Graduate School of Informatics, Nagoya University, Chikusa-ku, 464-8601 Nagoya, Japan*
[8] *Institute of Spintronics and Quantum Information, Faculty of Physics, Adam Mickiewicz University, 61-614 Poznań, Poland*
[9] *Dahlem Center for Complex Quantum Systems, Freie Universität Berlin, 14195 Berlin, Germany*
[10] *RIKEN Center for Quantum Computing (RQC), Wako-shi, Saitama 351-0198, Japan*
[11] *Department of Physics, The University of Michigan, Ann Arbor, 48109-1040 Michigan, USA*

(Dated: July 22, 2021)

Quantum channels, which break entanglement, incompatibility, or nonlocality, are not useful for entanglement-based, one-sided device-independent, or device-independent quantum information processing, respectively. Here, we show that such breaking channels are related to certain temporal quantum correlations, i.e., temporal separability, channel unsteerability, temporal unsteerability, and macrorealism. More specifically, we first define the steerability-breaking channel, which is conceptually similar to the entanglement and nonlocality-breaking channels and prove that it is identical to the incompatibility-breaking channel. Similar to the hierarchy relations of the temporal and spatial quantum correlations, the hierarchy of non-breaking channels is discussed. We then introduce the concept of the channels which break temporal correlations, explain how they are related to the standard breaking channels, and prove the following results: (1) A certain measure of temporal nonseparability can be used to quantify a non-entanglement-breaking channel in the sense that the measure is a memory monotone under the framework of the resource theory of the quantum memory. (2) A non-steerability-breaking channel can be certified with channel steering because the steerability-breaking channel is equivalent to the incompatibility-breaking channel. (3) The temporal steerability and non-macrorealism can, respectively, distinguish the steerability-breaking and the nonlocality-breaking unital channel from their corresponding non-breaking channels. Finally, a two-dimensional depolarizing channel is experimentally implemented as a proof-of-principle example to compare the temporal quantum correlations with non-breaking channels.

I. INTRODUCTION

The extension of quantum physics into the realm of information theory is important both for fundamental physics and for practical applications, such as quantum computing, quantum cryptography [1], and quantum random number generation [2, 3]. For the latter examples, the practical implementation of entangled based, device-independent, and one-side device-independent quantum information tasks [4–8] relies on the quantum resources, e.g., entangled [9–11], steerable [12–15], and nonlocal states [16–20], respectively. Extending these ideas to quantum networks [21–24], one needs reliable quantum devices (e.g., quantum communication lines [25] and quantum repeaters [26, 27]) to transmit or generate quantum resources between nodes (senders and receivers) in the network.

In general, the properties of quantum networks can be characterized by the concept of quantum channels [28], which is particularly convenient for estimating the preservability of quantum resources [29]. For instance, a reliable quantum memory [30–32] should ideally preserve the entanglement. Therefore, in the channel formalism, the most useful quantum memory is the identity channel, while the threshold of a quantum memory becoming useless is given by the entanglement-breaking (EB) channel [33, 34], which is also known as a measure-and-prepare channel. Obviously, quantum information tasks which rely on entanglement (e.g., the Ekert E91 cryptography protocol [4]) no longer work across the whole network once any part of the quantum network is EB.

Recently, the nonlocality-breaking (NLB) channels [35], defined in a similar way to the EB channel, were shown to be not useful for device-independent quantum information tasks. As expected from the hierarchy of correlations [36], the EB channel also breaks the nonlocality, but not vice versa [35, 37]. Thus, the EB channel is a strict subset of the set of NLB channels. Although the definition of the NLB channels is rigorous, one can only assess non-NLB channels by

* huan_yu@phys.ncku.edu.tw
† shin.liang.chen@phys.ncku.edu.tw
‡ yuehnan@mail.ncku.edu.tw

observing a Bell inequality violation with arbitrary entangled quantum states as input.

In order to detect a faithful quantum memory (i.e., detecting whether the equivalent channel is non-EB) with minimal assumptions, one can rely on a set of the temporal quantum correlations observed with an uncharacterized measurement apparatus [46] (see Fig. 1 for a schematic view of how to probe a non-breaking channel with the temporal quantum correlations). For instance, channel steering [13, 39], which is a generalization of standard spatial quantum steering, can be used to witness a non-EB channel. Moreover, a semi-quantum prepare-and-measure (SQPM) framework allows one to certify non-EB channels in a scenario where Alice received trusted quantum states as inputs [44]. Nevertheless, not all non-EB channels can be certified with channel steering. Later, the temporal semi-nonlocal game was proposed to witness "all" non-EB channels under the framework of a resource theory of quantum memories [38, 47]. This is done by expanding the concept of measurement-device-independent quantum information tasks into the temporal domain [48–51]. Another approach to assess the non-EB channel is by estimating the coherence of a state sent through the channel [45] while the used approach does not satisfy the memory monotone [38].

We here propose the concept of steerability-breaking (SB), which is not useful for one-sided device-independent quantum information tasks, and show that it is identical to the incompatibility-breaking channel [37]. Similar to the existing hierarchy relations in spatial and temporal quantum correlations [52, 53], the relationship between EB and NLB is discussed in Ref. [35]. Here, we further discuss the relationship between SB and NLB by showing that all NLB channels must be the SB channels. In addition, we show that the set of all Clauser-Horne-Shimony-Holt (CHSH) breaking channels [35, 54], which is a subset of all NLB channels, is a strict subset of all SB channels. Therefore, the hierarchy of breaking channels can be obtained.

We then connect the non-EB, non-SB, and non-NLB channels with certain temporal quantum correlations including the pseudo-density operator (PDO) [43], channel steerability [39], temporal steerability [40], and Leggett-Garg inequalities (LGIs) [55, 56] in the form of the temporal Bell inequality [41, 42, 57, 58]. More specifically, we show that: (1) a measure of the PDO satisfies the memory monotone [38], (2) channel steering can be used to certify all non-SB channels, while the temporal steerability can certify the non-SB unital channel, and (3) the temporal CHSH inequality violation can detect a non-CHSH-NLB unital channel. In Table I, we summarize some previous observations and our results of the breaking channels in the form of the temporal quantum correlations. We also experimentally study a 2-dimensional depolarizing channel as an explicit example to show the relationship between breaking channels and temporal quantum correlations.

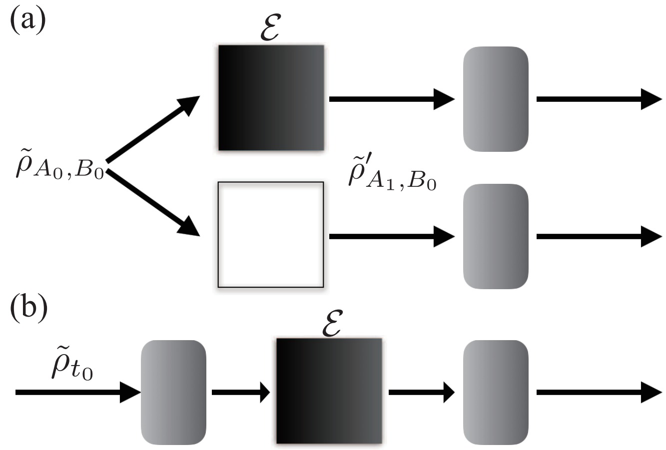

FIG. 1. Schematic illustration of certifying the quantum non-breaking channel with (a) spatial and (b) temporal quantum correlations. In (a), one relies on a bipartite quantum input $\tilde{\rho}_{A_0,B_0}$ sent to an unknown channel $\mathcal{E}$ (black box). The property of the channel can be probed by analyzing the obtained spatial correlation of the state $\tilde{\rho}'_{A_1,B_0}$ via a quantum measurement (grey rectangle). In (b), a given property of $\mathcal{E}$ can be probed by a temporal quantum correlation with an input $\tilde{\rho}_{t_0}$ which is measured before and after the channel.

II. QUANTUM CORRELATIONS AND THEIR CORRESPONDING BREAKING CHANNELS

In this section, we first briefly review the definitions and the properties of the EB and NLB channels. We then propose the SB channel, which is defined in analogy to the EB and NLB channels. The properties of the SB channel, including the relationship with the incompatibility-breaking channel, will also be discussed. Finally, we discuss the hierarchy relation for breaking channels.

Before showing our results, we first introduce some notations used in this work. We consider a Hilbert space H_A in a finite dimension d_A and $\mathcal{L}(H_A)$ the set of linear operators acting on H_A . We denote a set of standard density operators $\mathcal{D}(H_A) \in \mathcal{L}(H_A)$ satisfying the positive semidefiniteness and unit trace. A quantum channel is described by a set of complete-positive trace-preserving (CPTP) maps from $\mathcal{L}(H_A)$ to $\mathcal{L}(H_B)$ as $\mathcal{O}(H_A, H_B)$. The set of probability distributions is denoted as $\mathcal{P}(\mathcal{X})$ with a finite index set $\mathcal{X}$. Finally, we only consider the subsystem (say Alice without loss of generality) of the bipartite quantum state $\tilde{\rho}_{A_0,B_0} \in \mathcal{D}(H_{A_0}, H_{B_0})$ which is sent into the quantum channel $\mathcal{E} \in \mathcal{O}(H_{A_0}, H_{A_1})$, and denote the output state as $\tilde{\rho}'_{A_1,B_0} = (\mathcal{E} \otimes \mathbb{1})\tilde{\rho}_{A_0,B_0}$.

A. Quantum memory and entanglement-breaking channel

A bipartite quantum state $\tilde{\rho}_{A_0,B_0}$ shared between Alice and Bob is entangled if the corresponding density operator is not

Breaking channels	EB channel [33]	*SB channel* [37]	*unital SB channel* [37]	unital CHSH channel [35]
Spatial correlations	Entanglement	Steerability	Steerability	CHSH nonlocality
Temporal correlations	Temporal semi-nonlocal game* [38] *Temporal nonseparability** [43] Coherence [45]	*Channel steering* [39] *SQPM* [44]	*Temporal steering* [40]	*Temporal CHSH inequality* [41, 42]

TABLE I. Table showing how to probe non-breaking channels with spatial and temporal quantum correlations. Here the italics represent the results of this work and the asterisk marks the measures within the corresponding temporal scenarios satisfying the quantum memory monotone.

separable, namely

$$\tilde{\rho}_{A_0,B_0} \neq \sum_j p(j)\, \tilde{\sigma}^j_{A_0} \otimes \tilde{\eta}^j_{B_0}, \tag{1}$$

where $p(j) \in \mathcal{P}(\mathcal{J})$ is a probability distribution, and $\tilde{\sigma}^j_{A_0} \in \mathcal{D}(H_{A_0})$ ($\tilde{\eta}^j_{B_0} \in \mathcal{D}(H_{B_0})$) is a local density operator. In general, the EB channel is defined by sending Alice's subsystem into a quantum channel $\mathcal{E} \in O(H_{A_0}, H_{A_1})$, such that the entanglement is broken for arbitrary entangled states. We can explicitly formulate the EB channel as

$$\tilde{\rho}'_{A_1,B_0} = (\mathcal{E}^{\text{EB}} \otimes \mathbb{1})(\tilde{\rho}_{A_0,B_0}) = \sum_j p(j)\tilde{\sigma}^j_{A_1} \otimes \tilde{\eta}^j_{B_0}\ \ \forall\, \tilde{\rho}_{A_0,B_0}, \tag{2}$$

where $\tilde{\sigma}^j_{A_1} \in \mathcal{D}(H_{A_1})$. Here, the superscript EB is used to denote the channel $\mathcal{E}$ to be EB. The set of all EB channels is denoted by $\mathcal{EB}$.

Entanglement-breaking channels are equivalent to measure-and-prepare channels on a "single" quantum state. We use the terminology t_0 and t_1 (as well as their corresponding Hilbert space) to respectively denote a "single system" before and after the quantum channel. An EB channel $\mathcal{E}^{\text{EB}} \in O(H_{t_0}, H_{t_1})$ is alternatively expressed as

$$\mathcal{E}^{\text{EB}}(\tilde{\rho}_{t_0}) = \sum_j \text{Tr}\left[\tilde{\rho}_{t_0} M_j\right] \tilde{\sigma}^j_{t_1}, \tag{3}$$

where M_j is a positive-operator valued measurement (POVM) element satisfying $M_j > 0\ \forall\, j$ and $\sum_j M_j = \mathbb{1}$ with classical outcomes j. The physical interpretation of the EB channel can be explained as follows: one measures the original system $\tilde{\rho}_{t_0} \in \mathcal{D}(H_{t_0})$, after that, based on the outcome j, the corresponding state $\tilde{\sigma}^j_{t_1} \in \mathcal{D}(H_{t_1})$ is prepared. Obviously, when we send one of the entangled pairs into a measure-and-prepare channel, the system becomes separable since one has locally prepared another quantum state without any direct interaction with the other party.

It has been shown that the non-EB channel is the basic criterion for a functional quantum memory because one would like the quantum memory to, at the very least, preserve the entanglement in the state. Under the framework of the resource theory of quantum memory [38], the most general free operations of a quantum memory are the pre-quantum instruments and the post-quantum channels with the classical memory namely,

$$\Lambda(\mathcal{E}) = \sum_i D_i \circ \mathcal{E} \circ \mathcal{I}_i, \tag{4}$$

where $\Lambda(\mathcal{E})$ is a free transformation acting on the initial quantum channel $\mathcal{E}$. Here, D_i is a collection of quantum channels described by CPTP maps, and $\{\mathcal{I}_i\}$ is a quantum instrument satisfying CP, which sums up to CPTP. In Appendix A, we present a simple quantum memory monotone under these free operations.

B. Nonlocality-breaking channel

Before introducing the notion of the NLB channel, let us briefly recall the definition of Bell nonlocality. As discussed in the introduction, a spatially separated state is Bell-local when local measurements generate a correlation $p(a,b|x,y) = \text{Tr}\left[(M_{a|x} \otimes M_{b|y})\rho_{AB}\right]$ which admits a hidden variable (HV) model [17, 18], namely,

$$p(a,b|x,y) = \sum_j p(j)p(a|x,j)p(b|y,j), \tag{5}$$

where $\sum_j p(j)p(a|x,j)p(b|y,j)$ is the HV model with the correlations predetermined by a hidden variable j. Here, we denote a set of correlations admitting a HV model as $\mathcal{HV}$. Since $\mathcal{HV}$ is a convex set and quantum correlations are a strict superset of $\mathcal{HV}$, one can distinguish the local correlation from the quantum ones by testing the famous "Bell inequalities" given by the parameters $\beta^{x,y}_{a,b}$ [17, 18, 59], namely

$$B \equiv \sum_{a,b,x,y} \beta^{x,y}_{a,b}\, p(a,b|x,y)\ \leq\ \delta^{\beta}, \tag{6}$$

where δ^{β} is the local bound for a given Bell inequality.

Analogous to the EB channels, a NLB channel is the channel under which a correlation is obtained that always satisfies a given Bell inequality defined by $\beta^{x,y}_{a,b}$ in Eq. (6) for arbitrary measurements and states, namely [35]

$$\sum_{a,b,x,y} \beta^{x,y}_{a,b}\ \text{Tr}(M_{a|x} \otimes M_{b|y}\tilde{\rho}'_{A_1,B_0})\ \leq\ \delta^{\beta} \qquad \forall\, \{M_{a|x}\}, \{M_{b|y}\}, \tilde{\rho}_{A_0,B_0}. \tag{7}$$

We remark that deciding, whether a local hidden variable model exists for a given quantum state by testing every possible measurement, is a hard problem [60–62]. In Ref. [35], the authors considered the Clauser-Horne-Shimony-Holt (CHSH) NLB channel, which is a particular case of NLB channels which only considers the CHSH inequality [59], namely

$$B_{\text{CHSH}} \equiv E(x_1,y_1)+E(x_2,y_1)+E(x_1,y_2)-E(x_2,y_2) \leq 2, \quad (8)$$

where 2 is the local bound for the CHSH inequality, $E(x_i,y_j) \equiv p(a=b|x_i,y_j) - p(a \neq b|x_i,y_j)$ is the expectation value of $a \cdot b$, for $a \in \mathcal{A}$, $b \in \mathcal{B}$, $x_i \in \mathcal{X}$ and $y_j \in \mathcal{Y}$ with $\mathcal{X} = \mathcal{Y} = \{1,2\}$, and $\mathcal{A} = \mathcal{B} = \{\pm 1\}$. The quantum bound of the CHSH inequality is given by $2\sqrt{2}$. Unlike the situation in the EB scenario, the input of the maximally entangled state is not sufficient for verifying if the channel is CHSH-NLB [35, 63]. In this work, we are particularly interested in CHSH-NLB channels with the input being the maximally entangled state, denoted as *CHSH-NLB channels for the maximally entangled state*, since there are two important properties of such channels: (1) if the marginal of the input state is maximally mixed, then the state after channel cannot violate CHSH inequality and (2) if the channel is unital, then the channel is CHSH-NLB.

C. Steerability-breaking channels

In analogy to the EB and NLB channels, we propose a SB channel as a channel which breaks the steerability for any collection of measurements $\{M_{a|x}\}$ acting on the state sent through the channel. More specifically, by defining an assemblage as $\rho_{B_0}(a|x) \equiv \text{Tr}_{A_1}\left[(M_{a|x} \otimes \mathbb{1})\tilde{\rho}'_{A_1,B_0}\right]$, the assemblage after SB channel can always expressed as

$$\rho_{B_0}(a|x) = \sum_j p(j)p(a|x,j)\tilde{\sigma}^j_{B_0} \quad \forall \{M_{a|x}\}, \tilde{\rho}_{A_0,B_0}. \quad (9)$$

Here, $\sum_j p(j)p(a|x,j)\tilde{\sigma}^j_{B_0}$ is the hidden-state (HS) model consisting of the intrinsic states $\{\tilde{\sigma}^j_{B_0}\} \in \mathcal{D}(H_{B_0})$ with the classical postprocessing $p(j)p(a|x,j)$. The sets of all assemblages admitting HS model and all SB channels are denoted as $\mathcal{HS}$ and $\mathcal{SB}$, respectively. Moreover, we denote as $|\mathcal{X}|$-SB channels which break the steerability with a finite input $|\mathcal{X}|$. For instance, if the finite index set is $\mathcal{X} = \{1,2,3\}$, we can define the 3-SB channel. We note that the definition of the SB channel is similar to that of the incompatibility-breaking channel, which maps an incompatible measurement $\{M_{a|x}\}$ to a jointly measurable one in the Heisenberg picture [37, 64]. More specifically, a set of measurements after incompatibility-breaking channel can always expressed as

$$\mathcal{E}^\dagger(M_{a|x}) = \sum_\lambda p(a|x,\lambda)M_\lambda \quad \forall \{M_{a|x}\}, \quad (10)$$

where $\sum_\lambda p(a|x,\lambda)M_\lambda$ is a joint measurable model with an intrinsic POVM $\{M_\lambda\}$ and postprocessing $p(a|x,\lambda)$, and $\mathcal{E}^\dagger$ is the dual map of the quantum channel which is CP and unital. With the above definitions, we posit the following theorems:

Theorem 1. *A quantum channel is steerability-breaking if and only if it is also incompatibility-breaking.*

Proof.—We present the proof in Appendix B.

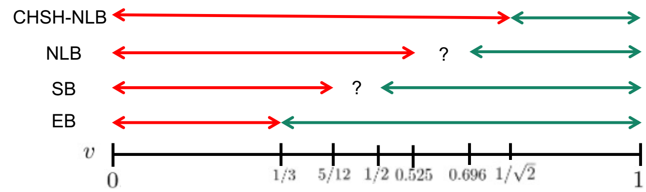

FIG. 2. Visibility parameter v for which the qubit depolarizing channel is CHSH-nonlocality breaking, nonlocality-breaking (NLB), steerability-breaking (SB), and entanglement-breaking (EB). The first bar in red represents the range, where the channel is proven to break the property, and the second bar in green shows the range, where the channel is proven not to break the property. The white areas with a question mark represent the ranges where the property is not known to be broken.

Although the definition of a SB channel is analogous to that of the EB channel, there is no simple way to characterize a set of SB channels, except for some explicit channels discussed in the literature [37]. It has already been shown that all EB channels can be certified with the maximally entangled input in Eq. (2) [33]. Here, we show that the SB channel also has the same property with the following theorem:

Theorem 2. *A quantum channel is steerability-breaking if and only if it breaks the steerability of a maximal entangled state.*

Proof.—We present the proof in Appendix B. The above property is useful not only for experimental-friendly certifications of the SB channel, but also for the theoretical analysis of the SB channel.

It has been shown that the set of all incompatibility-breaking channels (also the SB channel) and NLB channels are superset of all EB channels [35, 37]. Here, we also show the following:

Lemma 1. *The set of all SB channels is a strict superset of the all CHSH-NLB channels.*

Using the notes above, we arrive at the hierarchy in the breaking channels:

Theorem 3. *Similar to the hierarchy relation in temporal and spatial quantum correlations, the set of all non-EB, non-SB, non-NLB, and non-CHSH-NLB channels form a strict hierarchy. More specifically, we have the strict inclusions*

$$\mathcal{EB} \subset \mathcal{SB} \subset \mathcal{NLB} \subset \mathcal{NLB}_{\mathit{CHSH}}. \quad (11)$$

We present the proof of Theorem. 3 in Appendix D, and we illustrate this theorem for the qubit depolarizing channel

$$\mathcal{E}_{\text{D}}(v,\tilde{\rho}) = v\tilde{\rho} + (1-v)\frac{\mathbb{1}}{2} \quad (12)$$

in Fig. 2.

III. DETECTING QUANTUM NON-BREAKING CHANNELS WITH TEMPORAL QUANTUM CORRELATIONS

In this section, we present the results connecting EB, SB, and NLB channels with temporal separability, temporal non-steerability, and macrorealism. In section III A, we show that all EB channels are temporally separable and the measure of the temporal nonseparability satisfies the quantum memory monotone with an additional assumption. In section III B, we show that all the SB channels can be certified by testing the channel steerability. In section III C, the temporal steering and temporal Bell inequality are used to test whether the unital channel is SB and NLB, respectively.

A. Certifying non-EB channel with temporal quantum correlations

We first briefly recall the definition of the PDO, which has primarily been used in causality of quantum theory. We then show that a measure of temporal nonseparability extracted from a PDO satisfies the quantum "memory" monotone requirement as demanded by the framework of quantum memory resource theory. Afterwards, by considering the hierarchy in temporal correlations [53, 54], we show how to obtain the same probability distribution under the temporal semi-quantum game, which certifies the non-EB channel with minimal assumptions [38].

To reconstruct the state of a quantum system from observations or measurements performed at different times, one can generalize the concept of a standard density operator in the time domain [43]. Without loss of generality, the events, or observations, collated at different times can be connected by quantum channels with an input system. In what follows, we only consider a "two"-event PDO with the maximally mixed input. The information of a channel is contained in the PDO, namely [65]

$$R_{\mathcal{E}} = (\mathbb{1} \otimes \mathcal{E}) R_{\mathbb{1}}, \tag{13}$$

where $R_{\mathbb{1}} = \text{SWAP}/d$ is the PDO of the identity channel with the swap operator defined $\text{SWAP}|ij\rangle = |ji\rangle$. For the qubit case, we have $\text{SWAP} = 1/2 \sum_{i=0}^{3} \sigma_i \otimes \sigma_i$. Here, $\{\sigma_i\}_{i=0,1,2,3} = \{\mathbb{1}, \hat{X}, \hat{Y}, \hat{Z}\}$ is a set containing the identity and Pauli operators. A PDO is: (1) Hermitian and (2) unit trace but not necessarily positive semidefinite (the latter is a necessary condition for standard density operator). We note that although we only consider a qubit system above, the high-dimensional PDO can be trivially accessed [65]. Similar to the standard density operator, a PDO is called temporally separable when it admits

$$R_{\mathcal{E}} = \sum_j p(j)\, \tilde{\omega}_{t_0}^j \otimes \tilde{\theta}_{t_1}^j, \tag{14}$$

where $p(\lambda) \in \mathcal{P}(\mathcal{J})$, $\tilde{\omega}_{t_0}^j \in D(H_{t_0})$, and $\tilde{\theta}_{t_1}^j \in D(H_{t_1})$. We note that one cannot, in general, distinguish if the system is spatially or temporally separable when the PDO is positive semidefinite. Nevertheless, throughout this work, we refer to the correlation obtained as temporal correlation whenever there is no risk of ambiguity.

It has been shown that the PDO is identical to the partial transpose of the CJ state of the channel $\mathcal{E}$ [66, 67],

$$R_{\mathcal{E}}^{\text{PT}} = \tilde{\rho}_{\mathcal{E}}^{\text{CJ}}, \tag{15}$$

where PT is a partial transpose operation on the first subsystem. According to the positive partial transpose criterion, a separable PDO implies that the CJ state is also separable and thus the corresponding channel must be EB [68, 69]. With the above, we arrive at:

Lemma 2. *A PDO is separable if the corresponding channel is EB.*

Due to the hierarchy relation among temporal quantum correlations, we have the following:

Lemma 3. *Temporal steering and Leggett-Garg inequalities (LGIs)", in terms of the temporal Bell inequality without the classical memory, can be used to witness the non-EB channel with fewer assumptions.*

More precisely, since the set of PDOs admitting temporally separable models is a subset of the PDOs admitting the $\mathcal{HS}$ and $\mathcal{HV}$ models [53], temporal steering and temporal Bell inequality cannot be violated when the channel is EB, but not vice versa. Moreover, if temporal steering or a temporal Bell inequality is violated, the channel must be non-EB.

We now define a degree of temporal nonseparability by the f-function, namely [43]:

$$f = \frac{\|R_{\mathcal{E}}\| - 1}{2}, \tag{16}$$

where $\|X\| := \text{Tr}[\sqrt{XX^\dagger}]$ is the trace norm of an operation X. We recall that the set of free operations is given by $\Lambda(\mathcal{E}) = \sum_i D_i \circ \mathcal{E} \circ \mathcal{I}_i$ [38]. We show that the degree of temporal nonseparability is a quantum memory monotone.

Theorem 4. *A temporal nonseparability measure f is a convex quantum memory monotone.*

Proof.—We present the proof in Appendix A.

Finally, it is useful to compare the PDO and the temporal semi-nonlocal game, which certifies all the non-EB channels with minimal assumptions [38]. We consider a set of measurements $\{M_{a|x}\}$ at t_0 acting on the PDO which is used for generating a set of the density operators $\tilde{\rho}_{t_1}(a|x) \in \mathcal{D}(H_{t_1})$ at t_1 [53]. This is the so-called "normalized" temporal assemblage, and we will formally introduce it later. The joint measurement is performed with a characterized quantum input $\{\tilde{\tau}_y\} \in \mathcal{D}(H_{t_1})$ and the normalized temporal assemblage. The above steps are exactly identical to the procedure used in the temporal semi-nonlocal game, and we have

Lemma 4. *The PDO contains the statistical information of the temporal semi-nonlocal scenario.*

We present a detailed comparison in Appendix C. We note that, although in Ref. [54] the authors have already shown the relationship between the PDO and a temporal semi-nonlocal game, we provide a clearer physical interpretation in the proof by using the hierarchy relation in temporal quantum correlations.

B. Certifying non-SB channel with channel steering

Now we apply a set of uncharacterized measurements with a finite input $y \in \mathcal{Y}$ and outcome $b \in \mathcal{B}$ at time t_1 acting on the PDO which generates an "evolved" measurement $\{\mathcal{E}^\dagger(M_{b|y})\}$ by

$$\mathrm{Tr}_{t_0}\left[\mathbb{1} \otimes M_{b|y} R_{\mathcal{E}}\right] = \mathcal{E}^\dagger(M_{b|y})/d, \tag{17}$$

where d is the dimension of the PDO. Here, we only use the relation with the PDO and the CJ state in Eq. (15). Equation (17) is a valid assemblage and thus one can test whether Eq. (17) admits a HS model. Once the HS model is satisfied, the corresponding measurement set $\{\mathcal{E}^\dagger(M_{b|y})\}$ is jointly measurable (see also Appendix B). Therefore, once the dual channel breaks the incompatibility of an arbitrary measurement set $\{M_{b|y}\}$, the channel is SB by Theorem 1. The above description is a special case of channel steering [39, 46] with the trivial output of Bob. Note that the measurement at time t_0 is characterized and the classical memory can be used. From Theorem 1, we arrive at

Theorem 5. *All non-IB or non-SB channels can be certified in the temporal domain by violating the channel steering inequality.*

According to the definition of the PDO, Eq. (17) is experimental feasible. We note that all of the results in Refs. [39, 46] are also valid in our scenario.

C. Certifying unital non-SB and non-NLB channels for maximal entangled states with temporal correlations

In the temporal steering scenario, we currently consider the uncharacterized measurement with a finite input $x \in \mathcal{X}$ and outcome $a \in \mathcal{A}$ applied on the PDO at t_0. In the most general case, one can obtain a set of the subnormalized density operators, termed as a temporal assemblage [40, 70], namely

$$\rho_{\mathcal{E}}(a|x) = \mathrm{Tr}_{t_0}\left[M_{a|x} \otimes \mathbb{1} R_{\mathcal{E}}\right]. \tag{18}$$

In addition, since one often makes the noninvasive measurability assumption in the temporal steering scenario, the marginals of the temporal assemblage are independent of the classical input x, yielding the so-called no-signalling in time (NSIT) condition [71–74], namely $\sum_a \rho_{\mathcal{E}}(a|x) = \sum_a \rho_{\mathcal{E}}(a|x')$, $\forall\ x \neq x'$. We do not allow a classical memory, which sends classical information from t_0 to t_1, otherwise one can always have a temporal assemblage violating the HS model even when considering the EB channel [46]. We note that in the spatial quantum steering, the assemblage can also violate the HS model with classical communication from Alice to Bob [75]. For brevity, whenever there is no ambiguity we denote the assemblage $\{\rho_{\mathcal{E}}(a|x)\}$ as $\vec{\rho}$. It is convenient to quantify the degree of temporal steerability by the temporal steering robustness (TSR) [39, 62, 76], which refers to the minimum rate α of the noisy assemblage mixed with a given assemblage satisfying the HS model:

$$\mathrm{TSR}(\vec{\rho}) = \min\left\{\alpha | \frac{\rho_{\mathcal{E}}(a|x) + \alpha\sigma(a|x)}{1+\alpha} \in \mathcal{HS}\right\}. \tag{19}$$

Here, $\vec{\sigma}$ is an arbitrary assemblage. From Eqs. (15) and (18), one immediately sees that the temporal assemblage $\vec{\rho}_{\mathcal{E}}$ can be formulated

$$\rho_{\mathcal{E}}(a|x) = \mathcal{E}(M_{a|x})/d. \tag{20}$$

Because now the quantum channel is acting on the measurement, in what follows we only consider the unital quantum channel in the temporal steering scenario. We denote such a unital channel as $\mathcal{E}_{\text{unital}}$. It is easy to see that the set of quantum channels is a superset of the unital quantum channels. Obviously, if $\mathrm{TSR}(\vec{\rho}_{\mathcal{E}_{\text{unital}}}) = 0$ when considering an arbitrary measurement set $\{M_{a|x}\}$, the channel $\mathcal{E}_{\text{unital}}$ is a unital SB channel for the state $|\Phi_+\rangle$. Now, further considering Theorem 2, we can certify all unital SB channel with temporal steering. In other words, if one discovers $\mathrm{TSR}(\vec{\rho}_{\mathcal{E}}) \neq 0$, the unital channel $\mathcal{E}_{\text{unital}}$ is definitely non-SB. We then arrive at

Lemma 5. *Temporal steering can be used to certify all unital non-SB channels.*

Now, the measurements at t_1 are also replaced with a black box having finite inputs $y \in \mathcal{Y}$ and outcomes $b \in \mathcal{B}$ [41, 42, 56]. In other words, in the temporal Bell scenario, the measurements are both uncharacterized at t_0 and t_1. The temporal Bell inequality is defined as

$$B_{\mathrm{T}} \equiv \sum_{a,b,x,y} \beta^{x,y}_{a,b}\, p(a,b|x,y) \ \leq\ \delta^{\beta}_{\mathrm{T}}, \tag{21}$$

where $\delta^{\beta}_{\mathrm{T}}$ is the macrorealistic bound, and

$$\begin{aligned} p(a,b|x,y) &= \mathrm{Tr}\left[(M_{a|x} \otimes M_{b|y}) R_{\mathcal{E}}\right] \\ &= \mathrm{Tr}\left[M_{b|y}\rho_{\mathcal{E}}(a|x)\right]. \end{aligned} \tag{22}$$

If we find that $\langle B\rangle_{\mathrm{T}} \leq \delta^{\beta}_{\mathrm{T}}$, due to the macrorealistic assumption [55, 56], the physical quantity, referring to the probability here, is always determined by HV. The marginals of the probability cannot be influenced by the choice of the measurement apparatus at t_0 for satisfying the non-invasive measureability assumption or the NSIT condition [71, 72]. We note that similar to the communication loophole in the spatial Bell inequality [18], the classical memory is not allowed. One can immediately realize that certifying the macrorealistic probability distribution is identical to witnessing the locality of the CJ state (22). When Eq. (21) cannot be violated for arbitrary measurements, the channel breaks nonlocality for the maximally entangled states by definition. Alternatively, violating Eq. (21) implies the channel $\mathcal{E}$ is not NLB. Thus, we have

Lemma 6. *The LGI in terms of the temporal Bell inequality can be used to witness the non-NLB channel for the maximally entangled state.*

At the end of this section, we consider the CHSH-NLB channel and the "quantitative" temporal CHSH inequality, which optimize all possible measurement settings, namely

$$B_{\text{T-CHSH}}^{\max} = \max_{\{M_{a|x}\},\{M_{b|y}\}} \left\{ \frac{B_{\text{T-CHSH}} - 2}{2\sqrt{2} - 2}, 0 \right\}, \quad (23)$$

where $B_{\text{T-CHSH}}$ is the temporal CHSH inequality similar to Eq. (8), while the correlation is obtained temporally. Here, 2 and $2\sqrt{2}$ are the upper bounds of the temporal CHSH inequality under the HV model and quantum mechanics, respectively. Since the unital channel is CHSH-NLB when the channel breaks the CHSH nonlocality for the maximally entangled states, the temporal CHSH inequality can be used to certify all unital CHSH-NLB channels.

IV. EXPERIMENTAL SETUP AND RESULTS

In this section, we present a proof-of-principle experiment to see how the temporal quantum correlations can be applied to certify the breaking channels. In detail, we consider the 2-dimensional depolarizing channel which is a convex combination of white noise with the input state, namely,

$$\mathcal{E}_{\text{D}}(v, \tilde{\rho}) = v\tilde{\rho} + (1 - v)\frac{\mathbb{1}}{2}, \quad (24)$$

where v is the mixing parameter. The corresponding PDO can be expressed as

$$R_{\mathcal{E}_{\text{D}}} = \frac{v}{2}\text{SWAP} + \frac{1 - v}{4}\mathbb{1}, \quad (25)$$

In the temporal steering scenario, we consider the three dichotomic measurements ($\{\hat{X}, \hat{Y}, \hat{Z}\}$) applied on the PDO at t_0 in order to obtain the maximal temporal steerability [77, 78]. For the 2-dimensional depolarizing channel, the optimal measurement settings achieving the maximal violation of the temporal CHSH inequality are two sets of the anti-commuting measurements ($\{\hat{X}, \hat{Z}\}$ and $\{(\hat{X} + \hat{Z})/2, (\hat{X} - \hat{Z})/2\}$).

We have demonstrated all temporal scenarios in photonic experiments. The experimental setup is schematically shown in Fig. 3. In this experiment, qubits are encoded into the polarization state of individual photons and manipulated using linear optics. More details on the experimental implementation are provided in Appendix E.

A quarter and half-wave plates are used to prepare single photons in the desired polarization state. In our experiment, we prepared 10 different initial states which are the eigenstates of operators $\{\hat{X}, \hat{Y}, \hat{Z}\}$. This preparation is operationally equivalent to the nondestructive projective measurement at t_0. The photons then enter the depolarizing channel consisting of two beam displacer assemblies (BDA), one of which is enveloped by Hadamard gates ($\hat{H}$). These two BDAs together can perform one of following operations $\{\mathbb{1}, \hat{X}, \hat{Y}, \hat{Z}\}$. We assign each operation a probability depending on parameter v. To implement the depolarizing channel, we randomly (with assigned probabilities) with frequency 10 Hz change the operation and accumulate signal for sufficient enough time (100s) (see further details in Appendix E). To analyze the output state, we implement polarization projection and subsequent detection using a half and quarter-wave plate, a polarizer and a single photon detector. Note that the aforementioned half-wave plate is used to implement both the second Hadamard gate and the analysis.

Our experimental results are plotted in Fig. 4. As can be seen, the PDO is separable when $v \leq 1/3$ which saturates the bound of the EB channel in the quantum domain [38]. For the temporal steering and CHSH scenarios, the vanishing parameters v of the SB-breaking and CHSH-NLB channels in the quantum domain are $v = 1/\sqrt{3}$ and $1/\sqrt{2}$, respectively. We note that the temporal CHSH inequality is 0, when $v \leq 1/\sqrt{2}$ which is identical to the boundary of the CHSH-NLB channel under the 2-dimensional depolarizing channel [35, 63]. Moreover, the vanishing parameter for temporal steerability under the three measurement setting scenario is identical to that in the 3-incompatibility-breaking channel, which breaks the incompatibility of every collection of three measurements [37]. In other words, we can also say that it is the 3-SB channel which breaks the spatial steerability under all the three measurement settings. The error of all experimentally obtained quantities is estimated by assuming the Poisson distribution of the photon counts. Errors of quantities obtained from the density matrices is determined by a Monte-Carlo method. Numerical experimental results with errors are in Appendix E.

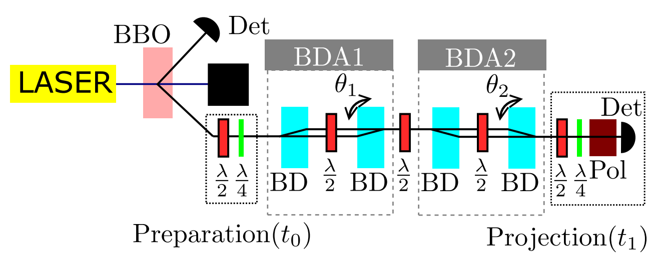

FIG. 3. Scheme for our experimental implementation of the depolarizing channel. The β-Ba$(BO_2)_2$ is a nonlinear crystal for spontaneous parametric down-conversion; $\lambda/2$ and $\lambda/4$ are half- and quarter-wave plates, respectively; BDs are beam displacers; BDAs are beam-displacer assemblies; Pol is a polarizer; and Det are single-photon detectors.

V. DISCUSSION

In this work, we have proposed the steerability-breaking (SB) channel, which is defined in an analogous way to the entanglement-breaking (EB) and nonlocality-breaking (NLB) channels. We have then proven a strict hierarchy between these concepts and illustrate it with the qubit depolarizing channel. In the Heisenberg picture, the set of the SB channels was shown to be equivalent to a previous concept of a

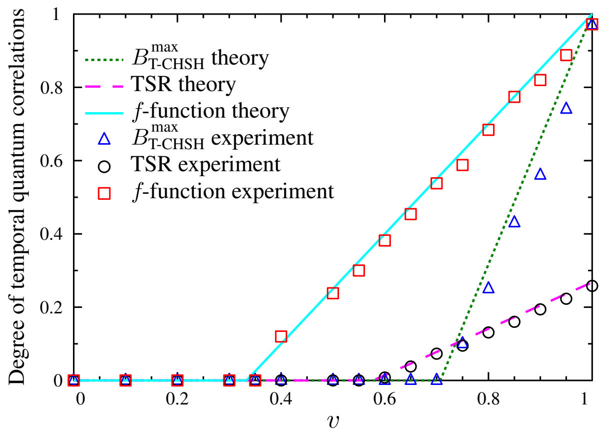

FIG. 4. Effects of the 2-dimensional depolarizing channel, characterized by the mixing parameter v in Eq. (24), on the TSR, f-function, and $B^{\max}_{\text{T-CHSH}}$ of a single qubit. Experimental (marked by symbols) vs theoretical predictions. The vanishing parameter of the f-function is $1/3$ which distinguishes the EB channel in the quantum domain. Moreover, for the temporal steering and CHSH scenarios, the vanishing parameters are respectively $1/\sqrt{3}$ and $1/\sqrt{2}$, which are the same as the boundaries of the 2-dimensional depolarizing channels for the SB and CHSH-NLB channels under the three and two dichotomic measurement settings.

incompatibility-breaking channel. We have shown the non-EB, and non-SB can be certified by the temporal inseparability and the channel steerability, respectively.

The temporal steerability and non-macrorealism can be applied to certify the unital non-SB and the unital non-CHSH-NLB channels, which only break the CHSH nonlocality instead of the general nonlocality. Therefore, the above breaking channels can be certified in the temporal scenarios without the entangled quantum input. We have also shown that the measure of the temporal nonseparability is a quantum memory monotone. We have also demonstrated the photonics experiment to explicitly show how temporal quantum correlations can be used to certify the non-breaking channels.

Several natural questions can be discussed: Can all the non-NLB channel be certified in the temporal scenario? Similar to the temporal semi-nonlocal game, which certify the non-EB channel in the measurement-device-independent scenario, the measurement-device-independent channel steering has been proposed [79] without considering the relation with the SB channel. We leave a systematic certifying the non-SB channel with the measurement-device-independent channel steering as an open problem.

ACKNOWLEDGMENTS

H.-Y. Ku and J. Kadlec contributed equally to this work. The authors acknowledge Karol Bartkiewicz for his help in numerical postprocessing of our experimental data. This work is supported partially by the National Center for Theoretical Sciences and Ministry of Science and Technology, Taiwan, Grants No. MOST 107-2628-M-006-002-MY3, and MOST 109-2627-E-006-004, and the Army Research Office (under Grant No. W911NF-19-1-0081). H.Y. acknowledges partial support from the National Center for Theoretical Sciences and Ministry of Science and Technology, Taiwan, Grants No. MOST 108-2811-M-006-536. MTQ acknowledges the Austrian Science Fund (FWF) through the SFB project BeyondC (sub-project F7103), a grant from the Foundational Questions Institute (FQXi) as part of the Quantum Information Structure of Spacetime (QISS) Project (qiss.fr). This project has received funding from the European Union's Horizon 2020 research and innovation programme under the Marie Skłodowska-Curie grant agreement No 801110 and the Austrian Federal Ministry of Education, Science and Research (BMBWF). It reflects only the authors' view, the EU Agency is not responsible for any use that may be made of the information it contains. N.L. acknowledges partial support from JST PRESTO through Grant No. JPMJPR18GC. A.M. is supported by the Polish National Science Centre (NCN) under the Maestro Grant No. DEC-2019/34/A/ST2/00081. F.N. is supported in part by: Nippon Telegraph and Telephone Corporation (NTT) Research, the Japan Science and Technology Agency (JST) [via the Quantum Leap Flagship Program (Q-LEAP) program, the Moonshot R&D Grant Number JPMJMS2061, and the Centers of Research Excellence in Science and Technology (CREST) Grant No. JPMJCR1676], the Japan Society for the Promotion of Science (JSPS) [via the Grants-in-Aid for Scientific Research (KAKENHI) Grant No. JP20H00134 and the JSPS-RFBR Grant No. JPJSBP120194828], the Army Research Office (ARO) (Grant No. W911NF-18-1-0358), the Asian Office of Aerospace Research and Development (AOARD) (via Grant No. FA2386-20-1-4069), and the Foundational Questions Institute Fund (FQXi) via Grant No. FQXi-IAF19-06. J.K. and K.L. acknowledge funding by Czech science Foundation (Grant No. 20-17765S) and by Palacky University (IGA_PrF_2021_004).

Appendix A: Quantum memory monotone

First, we recall the definition of a convex quantum memory monotone introduced in [38]. A quantum memory $Q(\mathcal{E})$ is a convex quantum memory monotone if it obeys the following conditions:

(i) It vanishes for free quantum memory:

$$Q(\mathcal{E}) = 0 \quad \text{if} \quad \mathcal{E} \ \text{is EB}. \tag{A1}$$

(ii) Q is non-increasing under the free operation, i.e.,

$$Q\left(\Lambda(\mathcal{E})\right) \leq Q(\mathcal{E}), \tag{A2}$$

where $\Lambda(X) = \sum_i D_i \circ X \circ \mathcal{I}_i$ is a free operation. Here, D_i is a collection of the CPTP maps, and $\mathcal{I}_i$ is a quantum instrument satisfying positivity and summed up to CPTP.

(iii) Given the classical mixture ($0 \leq \mu \leq 1$) of two channels ($\mathcal{E}_1$ and $\mathcal{E}_2$), the quality of the quantum memory satisfies the inequality

$$Q(\mu\mathcal{E}_1 + (1-\mu)\mathcal{E}_2) \leq \mu Q(\mathcal{E}_1) + (1-\mu)Q(\mathcal{E}_2). \tag{A3}$$

In what follows, we show that a measure of quantum casuality, denoted as a f-function, is a quantum memory monotone.

Lemma 7. *The value of the f-function is 0 when the channel is EB.*

Proof.— Since the CJ state of an EB channel must be separable, its corresponding PDO is also separable by Eq. (15). □

Before we prove that the f-function satisfies (ii), we show the following

Lemma 8. *Let $\Lambda : \mathcal{L}(H_1) \to \mathcal{L}(H_2)$ be a CP unital map and $\sigma \in \mathcal{L}(H_1)$ a positive semidefinite operator. It holds that*

$$\|\Lambda(\sigma)\| \leq \|\sigma\|. \tag{A4}$$

Proof.— The Stinespring dilation ensures that every unital CP map can be writen as $\Lambda(\sigma) = V^\dagger \left(\sigma \otimes \mathbb{1}_E\right) V$ where H_E is a linear space represented an environment E and $V : H_1 \to H_2$ is an isometry, *i.e.,* $V^\dagger V = \mathbb{1}$. Also, direct calculation shows that $VV^\dagger$ is an orthonormal projector, *i.e.,* $\left(VV^\dagger\right)^2 = VV^\dagger$ and $\left(VV^\dagger\right)^\dagger = VV^\dagger$. Since $\sigma \geq 0$ and Λ is CP we can write

$$\begin{aligned}
\|\Lambda(\sigma)\| &= \mathrm{tr}\left(\Lambda(\sigma)\right) \\
&= \mathrm{tr}\left(V^\dagger\sigma \otimes \mathbb{1} V\right) \\
&= \mathrm{tr}\left(VV^\dagger\sigma \otimes \mathbb{1}\right) \\
&= \mathrm{tr}\left(VV^\dagger\sigma \otimes \mathbb{1} VV^\dagger\right) \\
&= \|VV^\dagger\sigma \otimes \mathbb{1} VV^\dagger\|,
\end{aligned} \tag{A5}$$

where the last step holds true because $VV^\dagger\sigma \otimes \mathbb{1} VV^\dagger$ is positive semidefinite. If follows from Hölder inequality that

$$\|VV^\dagger\sigma \otimes \mathbb{1} VV^\dagger\| \leq \|VV^\dagger\|_\infty \, \|\sigma \otimes \mathbb{1}\| \, \|VV^\dagger\|_\infty \tag{A6}$$

where $\|.\|_\infty$ stands for the operator norm (the maximal singular value of an operator). Since all projectors have operator norm equals one, it holds that $\|\Lambda(\sigma)\| \leq \|\sigma\|$, finishing the proof. □

Lemma 9. *The f-function is decreasing under the free operation of the quantum memory.*

Proof.— Based on the definition of the f-function, we only need to show that the trace norm of the PDO under the operation $\Lambda(\mathcal{E}) = \sum_i D_i \circ \mathcal{E} \circ \mathcal{I}_i$ does not increase. We start by invoking Lemma 1 of Ref. [65] to write

$$\begin{aligned}
R_{\Lambda(\mathcal{E})} &= \mathbb{1} \otimes \sum_i D_i \circ \mathcal{E} \circ \mathcal{I}_i(R_{\mathbb{1}}) \\
&= \sum_i \mathcal{I}_i^\dagger \otimes D_i \circ \mathcal{E}(R_{\mathbb{1}}) \\
&= \sum_i \mathcal{I}_i^\dagger \otimes D_i(R_{\mathcal{E}}).
\end{aligned} \tag{A7}$$

Since $R_{\mathcal{E}}$ is hermitian, it admits the decomposition $R_{\mathcal{E}} = R_{\mathcal{E}}^+ - R_{\mathcal{E}}^-$, where $R_{\mathcal{E}}^\pm \geq 0$ have orthogonal support. This allows us to write

$$\begin{aligned}
\|R_{\Lambda(\mathcal{E})}\| &= \|\sum_i \mathcal{I}_i^\dagger \otimes D_i(R_{\mathcal{E}})\| \\
&= \|\sum_i \mathcal{I}_i^\dagger \otimes D_i(R_{\mathcal{E}}^+ - R_{\mathcal{E}}^-)\| \\
&= \|\sum_i \mathcal{I}_i^\dagger \otimes D_i(R_{\mathcal{E}}^+ - R_{\mathcal{E}}^-)\| \\
&\leq \|\sum_i \mathcal{I}_i^\dagger \otimes D_i(R_{\mathcal{E}}^+)\| + \|\sum_i \mathcal{I}_i^\dagger \otimes D_i(R_{\mathcal{E}}^-)\| \\
&= \mathrm{Tr}\left(\sum_i \mathcal{I}_i^\dagger \otimes D_i(R_{\mathcal{E}}^+)\right) + \mathrm{Tr}\left(\sum_i \mathcal{I}_i^\dagger \otimes D_i(R_{\mathcal{E}}^-)\right) \\
&= \mathrm{Tr}\left(\sum_i \mathcal{I}_i^\dagger \otimes \mathbb{1}(R_{\mathcal{E}}^+)\right) + \mathrm{Tr}\left(\sum_i \mathcal{I}_i^\dagger \otimes \mathbb{1}(R_{\mathcal{E}}^-)\right) \\
&= \|\sum_i \mathcal{I}_i^\dagger \otimes \mathbb{1}(R_{\mathcal{E}}^+)\| + \|\sum_i \mathcal{I}_i^\dagger \otimes \mathbb{1}(R_{\mathcal{E}}^-)\|.
\end{aligned} \tag{A8}$$

Now, since $\sum_i \mathcal{I}_i$ is TP, we have that $\sum_i \mathcal{I}_i^\dagger$ is unital, hence we can invoke Lemma 8 to ensure that

$$\|\sum_i \mathcal{I}_i^\dagger \otimes \mathbb{1}(R_{\mathcal{E}}^+)\| + \|\sum_i \mathcal{I}_i^\dagger \otimes \mathbb{1}(R_{\mathcal{E}}^-)\| \leq \|R_{\mathcal{E}}^+\| + \|R_{\mathcal{E}}^-\|. \tag{A9}$$

We now finish the proof by pointing that, since $R_{\mathcal{E}}^+$ and $R_{\mathcal{E}}^-$ have orthogonal support, it holds that

$$\begin{aligned}
\|R_{\mathcal{E}}^+\| + \|R_{\mathcal{E}}^-\| &= \|R_{\mathcal{E}}^+ - R_{\mathcal{E}}^-\| \\
&= \|R_{\mathcal{E}}\|. \square
\end{aligned} \tag{A10}$$

Lemma 10. *The f-function satisfies the property (iii).*

Proof.— The proof has been shown in Ref. [43].

With the above lemmas, we complete the Theorem 4 in the main text.

Appendix B: The set of the steerability-breaking channels is identical to the set of the incompatibility-breaking channel.

We first summarize that the following statements are equivalent related to a quantum channel $\mathcal{E}$:

#1. A quantum channel breaks the steerability for any arbitrary quantum state $\tilde{\rho}_{AB}$ and arbitrary measurement set $\{M_{a|x}\}$.

#2. A quantum channel breaks the steerability for the maximally entangled states and arbitrary measurement set $\{M_{a|x}\}$.

#3. A dual of the quantum channel $\mathcal{E}^\dagger$ breaks the incompatibility for the arbitrary measurement set $\{M_{a|x}\}$. In the other words, $\mathcal{E}^\dagger(M_{a|x})$ is joint measurable.

Lemma 11. *The above-mentioned statements #2 and #3 are equivalent.*

Proof.—For #3⇒ #2, it is trivial because the incompatible measurement is a necessary condition for demonstrating the steerability [80, 81]. If the channel is incompatibility-breaking, it must also be steerability breaking. For #2⇒# 3, we consider the state $\tilde{\rho}_{A,B}=|\Phi\rangle\langle\Phi|$ with $|\Phi\rangle=\frac{1}{d}\sum_{i=1}^{d}|i\rangle\otimes|i\rangle$, and arbitrary measurement set $\{M_{a|x}\}$. The corresponding assemblage can be obtained by

$$\begin{aligned}\mathrm{Tr}_A&\left[(M_{a|x}\otimes\mathbb{1})(\mathcal{E}\otimes\mathbb{1})|\Phi\rangle\langle\Phi|\right]\\&=\mathrm{Tr}_A\left[(\mathcal{E}^\dagger(M_{a|x})\otimes\mathbb{1})|\Phi\rangle\langle\Phi|\right]\\&=\frac{1}{d}\left[\mathcal{E}^\dagger(M_{a|x})\right]^{\mathrm{T}}.\end{aligned}\tag{B1}$$

Since the assemblage itself must satisfy a HS model, we can reformulate the above as

$$\begin{aligned}\left[\mathcal{E}^\dagger(M_{a|x})\right]^{\mathrm{T}}&=d\times\sum_\lambda p(a|x,\lambda)p(\lambda)\tilde{\rho}_\lambda\\&=\sum_\lambda p(a|x,\lambda)M_\lambda.\end{aligned}\tag{B2}$$

By summing up the outcome a in Eq. (B2)

$$\begin{aligned}\mathbb{1}\equiv\sum_a\left[\mathcal{E}^\dagger(M_{a|x})\right]^{\mathrm{T}}&=\sum_{a,\lambda}p(a|x,\lambda)M_\lambda\\&=\sum_\lambda M_\lambda,\end{aligned}\tag{B3}$$

we can show $M_\lambda=dp(\lambda)\tilde{\rho}_\lambda$ is a valid POVM. Here, we use the facts that $\left[\mathcal{E}^\dagger(M_{a|x})\right]^{\mathrm{T}}$ is a valid POVM and $\sum_a\left[\mathcal{E}^\dagger(M_{a|x})\right]^{\mathrm{T}}=\mathbb{1}$. Therefore, the last equation in Eq. (B2) is joint measurable. From above, we prove #2⇔#3. □

Lemma 12. *The above-mentioned statements #1 and #3 are equivalent.*

Proof.— Since #3⇒#1 is trivial, we are going to show #1⇒ #3. An equivalent description of #1⇒#3 is (≠ #3)⇒ (≠ #1). According to the definition of the incompatibility-breaking channel, there exists a set of measurements $\{M_{a|x}\}$ such that the "evolved" measurement $\{\mathcal{E}^\dagger(M_{a|x})\}$ is incompatible. Now, if we consider Alice and Bob sharing a maximally entangled state $\tilde{\rho}_{A,B}=|\Phi\rangle\langle\Phi|$ with $|\Phi\rangle=\frac{1}{d}\sum_{i=1}^{d}|i\rangle\otimes|i\rangle$, we can obtain the following assemblage which is the same as Eq. (B1). Since $\frac{1}{d}\left[\mathcal{E}^\dagger(M_{a|x})\right]^{\mathrm{T}}$ must be steerable, the channel is not a SB channel by definition. □

Although from above two Lemmas, it is enough to show that the statements #1, #2, and #3 are equivalent. We still provide an independent proof of #2⇔#3.

Lemma 13. *The above-mentioned #1 and #2 are equivalent.*

Proof.— By definition, #1⇒#2 is trivial. In the following, we show that #2⇒#1 also holds. First, we introduce the maximally entangled state $|\Phi\rangle\langle\Phi|=\frac{1}{d}\sum_{i,j}|i\rangle\langle j|\otimes|i\rangle\langle j|$, the hidden state $\tilde{\rho}^\lambda=\sum_{i,j}\chi_{i,j}^\lambda|i\rangle\langle j|$, and the arbitrary bipartite quantum state $\tilde{\tau}=\sum_{mnpq}\Upsilon_{p,q}^{m,n}|m\rangle\langle n|\otimes|p\rangle\langle q|$ in the matrix representation. Here $\chi_{i,j}^\lambda$ and Υ_{mnpq} are the entries of the corresponding states. From #2, there must exist a hidden state model for the channel $\mathcal{E}$ breaking the steerability of the maximally entangled state for arbitrary measurement set $\{E_{a|x}\}$ and we have

$$\begin{aligned}&\mathrm{Tr}_A\left[(E_{a|x}\otimes\mathbb{1})(\mathcal{E}\otimes\mathbb{1})|\Phi\rangle\langle\Phi|\right]=\\&\frac{1}{d}\sum_{i,j}\mathrm{Tr}\left[E_{a|x}\mathcal{E}(|i\rangle\langle j|)\right]|i\rangle\langle j|=\\&\sum_\lambda p(a|x,\lambda)p(\lambda)\tilde{\rho}^\lambda=\\&\sum_{i,j,\lambda}p(a|x,\lambda)p(\lambda)\chi_{i,j}^\lambda|i\rangle\langle j|.\end{aligned}\tag{B4}$$

By linearity, we obtain

$$\mathrm{Tr}\left[E_{a|x}\mathcal{E}(|i\rangle\langle j|)\right]=d\sum_\lambda p(a|x,\lambda)p(\lambda)\chi_{i,j}^\lambda.\tag{B5}$$

Now, inserting the arbitrary bipartite state into the definition of the SB channel, one finds

$$\begin{aligned}\mathrm{Tr}_A\left[\mathcal{E}^\dagger(E_{a|x})\otimes\mathbb{1}\tilde{\tau}\right]&=\sum_{m,n,p,q}\Upsilon_{p,q}^{m,n}\mathrm{Tr}\left[E_{a|x}\mathcal{E}(|m\rangle\langle n|)\right]|p\rangle\langle q|\\&=\sum_{m,n,p,q}\Upsilon_{p,q}^{m,n}(d\sum_\lambda p(a|x,\lambda)p(\lambda)\chi_{i,j}^\lambda)|p\rangle\langle q|\\&=d\sum_\lambda p(a|x,\lambda)p(\lambda)\sum_{m,n,p,q}\Upsilon_{p,q}^{m,n}\chi_{i,j}^\lambda|p\rangle\langle q|\\&=d\sum_\lambda p(a|x,\lambda)p(\lambda)\mathrm{Tr}_A\left[\tilde{\tau}(\mathbb{1}\otimes(\tilde{\rho}^\lambda)^T)\right].\end{aligned}\tag{B6}$$

It is trivial to see that $\mathrm{Tr}_A\left[\tilde{\tau}(\mathbb{1}\otimes(\tilde{\rho}^\lambda)^T)\right]$ is positive semidefinite. Now the remaining problem is to show that $d\mathrm{Tr}_A\left[\tilde{\tau}(\mathbb{1}\otimes(\tilde{\rho}^\lambda)^T)\right]$ is a valid quantum state. Since the LHS of Eq. (B6) is a valid assemblage, the marginal assemblage is a valid quantum state with unit trace. Thus, we trace the marginal assemblage on the RHS and obtain

$$\begin{aligned}&\sum_a\mathrm{Tr}\left[(E_{a|x}\otimes\mathbb{1})(\mathcal{E}\otimes\mathbb{1})\tilde{\tau}\right]=\\&\quad d\sum_{a,\lambda}p(a|x,\lambda)p(\lambda)\mathrm{Tr}\left[\tau(\mathbb{1}\otimes(\tilde{\rho}^\lambda)^T)\right]=\\&\quad d\sum_\lambda p(\lambda)\mathrm{Tr}\left[\tilde{\tau}(\mathbb{1}\otimes(\tilde{\rho}^\lambda)^T)\right]\equiv1.\end{aligned}\tag{B7}$$

Since $\sum_\lambda p(\lambda)=1$, and $\mathrm{Tr}\left[\tilde{\tau}\right]=\mathrm{Tr}\left[(\tilde{\rho}^\lambda)^T\right]=1$, the only choice for satisfying above is $d\mathrm{Tr}\left[\tau(\mathbb{1}\otimes(\tilde{\rho}^\lambda)^T)\right]=1$, with arbitrary states $\tilde{\tau}$ and $(\tilde{\rho}^\lambda)^T$. Thus, $d\mathrm{Tr}_A\left[\tilde{\tau}(\mathbb{1}\otimes(\tilde{\rho}^\lambda)^T)\right]$ is a valid assemblage. With above we complete #2⇔#3.□

Appendix C: From PDO to the temporal semi-quantum game

The temporal semi-quantum game considers two players, Alice and Bob. They are able to generate the same set of characterized quantum states $\{\tilde{\sigma}_x\} \in \mathcal{D}(H_A)$ and $\mathcal{D}(H_B)$ with the finite number set $x \in \mathcal{X}$ and $y \in \mathcal{Y}$. Alice first sends a state $\tilde{\sigma}_x$ from the set into a quantum channel $\mathcal{E}$. After the channel, Bob performs a joint measurement B_b with the evolved state and the second quantum input sending from Bob. Here, b is the observed measurement outcome. To certify all non-EB channels, the set of quantum states should form a tomographically complete set, e.g., the eigenstates of the Pauli matrices.

To show the results in this section, it is convenient for compactly reformulating the joint measurement with the quantum input at t_1 as $M_b = \mathrm{Tr}_B(B_b(\mathbb{1} \otimes \tilde{\sigma}_y))$, which forms an effective POVMs. Following the Born's rule, the probability distribution obtained can be expressed as

$$p(b|x,y) = \mathrm{Tr}\left[B_b \tilde{\sigma}_y \otimes \mathcal{E}(\tilde{\sigma}_x)\right] = \mathrm{Tr}\left[M_b \mathcal{E}(\tilde{\sigma}_x)\right]. \quad \text{(C1)}$$

Now, we show how to obtain the same probability distribution from the causality quantity PDO $R_{\mathcal{E}}$. First, we recall that the normalized quantum states at time t_1 can be obtained by applying a set of measurements $\{M_x\}$ at t_0 in Eq. (18) with normalization [53]. More specifically, the effect of the measurement at t_0 on PDO generates the evolved postmeasurement states at t_1. Finally the measurement M_b at t_1 is implemented, and we can obtain the same probability distribution in the temporal semi-quantum game.

Appendix D: Proof of the hierarchy in quantum non-breaking channels

According to the definitions in Eqs. (7) and (9), one can trivially see that the set of all SB channels must be NLB [14]. Thus, we have $\mathcal{SB} \subseteq \mathcal{NLB}$. To show that the hierarchy is indeed strict, we consider the single-qubit depolarising channel defined in Eq. (24). It is known that the qubit depolarizing channel is EB if and only if $v \leq 1/3$ and that it is CHSH-NLB if and only if $v \leq 1/\sqrt{2}$ [35]. The two-qubit isotropic state

$$\mathrm{ISO}_v = v|\phi^+\rangle\phi^+ + (1-v)\mathbb{1}/4 \quad \text{(D1)}$$

is steerable (with projective measurements) when $v > 1/2$ [14], hence, due to Theorem 2, the qubit isotropic channel is not SB for $v > 1/2$. Also, for $v \leq 5/12$, the isotropic state is unsteerable for any POVM [37, 52]; hence $v \leq 5/12$ ensures SB.

The two-qubit isotropic state violates a Bell inequality when $v > 0.696$ [82]. Hence the depolarizing channel cannot be NLB in this range. In order to prove that a quantum channel is NLB, we make use of a local hidden variable for quantum measurements [83]. Reference [84] shows that for any set of qubit measurements $\{M_{a|x}\}$, when $v \leq 0.525$, the set of the measurements

$$\{vM_{a|x} + (1-v)\mathrm{Tr}(M_{a|x})\mathbb{1}/2\} \quad \text{(D2)}$$

admits a local hidden variable model. That is, for any bipartite quantum state, when $v \leq 0.525$, if Alice performs this set of noise measurements, the statistics are necessarily Bell local. Since the depolarizing channel is self-dual ($\mathcal{E}_D = \mathcal{E}_D^\dagger$), the qubit depolarizing channel is NLB when $v \leq 0.525$. □

Appendix E: Experimental implementation details and data

As a source of horizontally polarized discrete photons, we use a type-I process of spontaneous parametric down-conversion. One photon from each pair serves as a herald while the other one enters the experimental setup. More specifically, a Coherent Paladin laser at 355 nm is used to pump a β-Ba(BO$_2$)$_2$ crystal which produces two photons at 710 nm. In this experiment, we employ polarization encoding associating the horizontal and vertical polarization with the logical states $|0\rangle$ and $|1\rangle$, respectively.

For realizing the depolarizing channel, we consider the following Kraus representation,

$$\tilde{\mathcal{E}}_\mathrm{D}(p,\tilde{\rho}) = p\tilde{\rho} + \frac{(1-p)}{3}(\hat{X}\tilde{\rho}\hat{X} + \hat{Y}\tilde{\rho}\hat{Y} + \hat{Z}\tilde{\rho}\hat{Z}), \quad \text{(E1)}$$

where p parameterizes the channel. As one can see, there is a linear transformation between the above formula and the one in Eq. (24) via $p = (3v+1)/4$. The depolarizing channel (Fig. 3) is implemented by means of two beam displacer assemblies (BDA1 and BDA2). A beam displacer assembly consists of two beam displacers and a half-wave plate in between. The horizontally and vertically polarized parts of the wave packet are displaced on the first beam displacer, then the polarizations are swapped on the half-wave plate and finally beams are rejoined at the second beam displacer. By slightly tilting the second beam displacer, which is mounted on a piezo actuator, we introduce a phase shift θ_i (where i indexes the two beam displacer assemblies) between the horizontal and vertical component of the photon's polarization state.

The role of the first beam displacer assembly (BDA1) is to implement either the $\mathbb{1}$ or the $\hat{Z}$ (phase flip) operation depending on whether the introduced phase shift is $\theta_1 = 0$ or $\theta_1 = \pi$, respectively. The second beam displacer assembly (BDA2) is enveloped by two half-wave plates (rotated by 22.5° with respect to the horizontal polarization), each serving as a Hadamard gate ($\hat{H}$). The overall effect of the second beam displacer together with these gates is the implementation of either $\mathbb{1}$ or the $\hat{X} = \hat{H}\hat{Z}\hat{H}$ (bit flip) operation, provided we set the phase shift to $\theta_2 = 0$ or $\theta_2 = \pi$, respectively. Note that the remaining operation is implemented as a product of both beam displacer assembly actions $\hat{Y} = i\hat{X}\hat{Z}$ ($\theta_1 = \theta_2 = \pi$).

To depolarize the photon state as prescribed in Eq. (E1) we generate, with frequency f_r, random real number $r \in [0,1]$ (uniformly distributed). Based on the value of r, we choose the setting of θ_1 and θ_2 (see Table II).

To analyze the output state, we implement the polarization projection and subsequent detection using a half and quarter-wave plate, a polarizer, and a single-photon detector. Note that the aforementioned half-wave plate is used to implement both the second Hadamard gate and the analysis. The measured signal, for any combination of prepared and projected states, is integrated over a period $T \gg 1/f_r$. In our experiment, we accumulate the number of heralded photon detections for $T = 100$ s using $f_r = 10$ Hz.

TABLE II. Phase shifts and operations assigned to randomly generated numbers.

r in range	θ_1	θ_1	Operation
$[0, p]$	0	0	$\mathbb{1}$
$\left(p, p + \frac{(1-p)}{3}\right]$	π	0	$\hat{Z}$
$\left(p + \frac{(1-p)}{3}, p + \frac{2(1-p)}{3}\right]$	0	π	$\hat{X}$
$\left(p + \frac{2(1-p)}{3}, 1\right]$	π	π	$\hat{Y}$

In the experiment, we prepared 10 different initial states, eigenstates of operators $\{\hat{X}, \hat{Y}, \hat{Z}, (\hat{X} + \hat{Z}), (\hat{X} - \hat{Z})\}$ and projected them onto the same set of states. We have thus registered photon counts for all 100 combinations of prepared and projected states. For subsequent data processing, we did not use data from all 100 combinations of prepared and projected states.

From the 36 measurements corresponding to the projections onto the eigenstates of the Pauli operators $\{\hat{X}, \hat{Y}, \hat{Z}\}$ as, both preparation states and projection states, we calculated the Choi-Jamiołkowski matrix, using the maximum likelihood estimation [85]. From this matrix, we calculated the f-function (16) (marked by □ in Fig. 4) and purity of the process.

From the same set of 36 measurements, we calculated the assemblages $\rho_{\mathcal{E}}(a|x)$. In this case, for each of the 6 preparation states, we obtained a full output state tomography based on the 6 projection states, and the single-qubit density matrices were estimated by maximum likelihood [86]. Due to experimental imperfections, these matrices slightly violate the no-signalling condition, which is expressed as

$$\sum_a \rho_{\mathcal{E}}(a|x) = \sum_a \rho_{\mathcal{E}}(a|x')\ \forall\, x, x'. \tag{E2}$$

To solve this issue, we use semidefinite programming to find assemblages $\{\tilde{\rho}_{\mathcal{E}}(a|x)\}$, that fulfil the no-signaling condition, such that the sum of the fidelities of the original unphysical assemblages violating the condition and the physical ones $\{\tilde{\rho}_{\mathcal{E}}(a|x)\}$ is maximized.

The minimal fidelity across all parameters v and all the assemblages is 99.88%. Using these newly found assemblages, we calculated the temporal steering robustness (19) (○ in Fig. 4).

For the calculation of the temporal CHSH inequality (23), we used the measurements with states prepared in eigenstates of $\{\hat{X}, \hat{Z}\}$ together with projections onto eigenstates of $\{(\hat{X} + \hat{Z}), (\hat{X} - \hat{Z})\}$ (△ in Fig. 4).

The details of the experimental results are presented in Tables II and III.

TABLE III. Summary of our experimental results.

v	$B^{\max}_{\text{T-CHSH}}$	TSR	f-function	purity
0.00(1)	0.00(0)	0.000(0)	0.000(0)	0.255(1)
0.10(1)	0.00(0)	0.000(0)	0.000(0)	0.273(1)
0.20(1)	0.00(0)	0.000(0)	0.000(0)	0.290(2)
0.30(1)	0.00(0)	0.000(0)	0.000(0)	0.332(2)
0.35(1)	0.00(0)	0.000(0)	0.00(4)	0.338(2)
0.40(1)	0.00(0)	0.000(0)	0.120(6)	0.381(3)
0.50(1)	0.00(0)	0.000(0)	0.238(6)	0.434(3)
0.55(1)	0.00(0)	0.000(0)	0.300(6)	0.467(4)
0.60(1)	0.00(0)	0.008(2)	0.382(6)	0.514(3)
0.65(1)	0.00(0)	0.038(2)	0.454(6)	0.557(4)
0.70(1)	0.00(0)	0.073(2)	0.538(6)	0.612(4)
0.75(1)	0.10(4)	0.095(2)	0.588(4)	0.648(4)
0.80(1)	0.25(4)	0.131(2)	0.684(6)	0.721(4)
0.85(1)	0.43(4)	0.160(2)	0.774(4)	0.766(4)
0.90(1)	0.56(4)	0.194(1)	0.820(4)	0.832(3)
0.95(1)	0.74(4)	0.223(1)	0.888(4)	0.893(3)
1.00(0)	0.97(3)	0.258(1)	0.972(1)	0.972(1)

[1] N. Gisin, G. Ribordy, W. Tittel, and H. Zbinden, *Quantum cryptography*, Rev. Mod. Phys. **74**, 145 (2002).

[2] M. Herrero-Collantes and J. C. Garcia-Escartin, *Quantum random number generators*, Rev. Mod. Phys. **89**, 015004 (2017).

[3] B. Sanguinetti, A. Martin, H. Zbinden, and N. Gisin, *Quantum Random Number Generation on a Mobile Phone*, Phys. Rev. X **4**, 031056 (2014).

[4] A. K. Ekert, *Quantum cryptography based on Bell's theorem*, Phys. Rev. Lett. **67**, 661 (1991).

[5] A. Acín, N. Brunner, N. Gisin, S. Massar, S. Pironio, and V. Scarani, *Device-Independent Security of Quantum Cryptography against Collective Attacks*, Phys. Rev. Lett. **98**, 230501 (2007).

[6] Y. Liu, Q. Zhao, M.-H. Li, J.-Y. Guan, Y. Zhang, B. Bai, W. Zhang, W.-Z. Liu, C. Wu, X. Yuan, H. Li, W. J. Munro, Z. Wang, L. You, J. Zhang, X. Ma, J. Fan, Q. Zhang, and J.-W. Pan, *Device-independent quantum random-number generation*, Nature **562**, 548 (2018).

[7] C. Branciard, E. G. Cavalcanti, S. P. Walborn, V. Scarani, and H. M. Wiseman, *One-sided device-independent quantum key distribution: Security, feasibility, and the connection with steering*, Phys. Rev. A **85**, 010301 (2012).

[8] K. Sun, X.-J. Ye, Y. Xiao, X.-Y. Xu, Y.-C. Wu, J.-S. Xu, J.-L. Chen, C.-F. Li, and G.-C. Guo, *Demonstration of Einstein–Podolsky–Rosen steering with enhanced subchannel discrimination*, npj Quantum Inf. **4** (2018).

[9] R. Horodecki, P. Horodecki, M. Horodecki, and K. Horodecki, *Quantum entanglement*, Rev. Mod. Phys. **81**, 865 (2009).

[10] O. Gühne and G. Tóth, *Entanglement detection*, Physics Reports **474**, 1 (2009).

[11] S.-H. Chen, M.-L. Ng, and C.-M. Li, *Quantifying entanglement preservability of experimental processes*, (2020), arXiv:2006.05346 [quant-ph].
[12] E. Schrödinger, *Discussion of Probability Relations between Separated Systems*, Proc. Cambridge Phil. Soc. **31**, 555 (1935).
[13] R. Uola, A. C. S. Costa, H. C. Nguyen, and O. Gühne, *Quantum steering*, Rev. Mod. Phys. **92**, 015001 (2020).
[14] H. M. Wiseman, S. J. Jones, and A. C. Doherty, *Steering, Entanglement, Nonlocality, and the Einstein-Podolsky-Rosen Paradox*, Phys. Rev. Lett. **98**, 140402 (2007).
[15] S.-H. Chen, Y.-C. Kao, N. Lambert, F. Nori, and C.-M. Li, *Nonclassical Preparation of Quantum Remote States*, (2020), arXiv:2008.06238 [quant-ph].
[16] A. Einstein, B. Podolsky, and N. Rosen, *Can Quantum-Mechanical Description of Physical Reality Be Considered Complete?*, Phys. Rev. **47**, 777 (1935).
[17] J. S. Bell, *On the Einstein-Podolsky-Rosen Paradox*, Physics **1**, 195 (1964).
[18] N. Brunner, D. Cavalcanti, S. Pironio, V. Scarani, and S. Wehner, *Bell nonlocality*, Rev. Mod. Phys. **86**, 419 (2014).
[19] S.-H. Chen, H. Lu, Q.-C. Sun, Q. Zhang, Y.-A. Chen, and C.-M. Li, *Discriminating quantum correlations with networking quantum teleportation*, Phys. Rev. Research **2**, 013043 (2020).
[20] T. Kriváchy, Y. Cai, D. Cavalcanti, A. Tavakoli, N. Gisin, and N. Brunner, *A neural network oracle for quantum nonlocality problems in networks*, npj Quantum Inf. **6**, 70 (2020).
[21] Y. Wang, I. W. Primaatmaja, E. Lavie, A. Varvitsiotis, and C. C. W. Lim, *Characterising the correlations of prepare-and-measure quantum networks*, npj Quantum Inf. **5**, 17 (2019).
[22] J. F. Dynes, A. Wonfor, W. W. S. Tam, A. W. Sharpe, R. Takahashi, M. Lucamarini, A. Plews, Z. L. Yuan, A. R. Dixon, J. Cho, Y. Tanizawa, J. P. Elbers, H. Greißer, I. H. White, R. V. Penty, and A. J. Shields, *Cambridge quantum network*, npj Quantum Inf. **5**, 101 (2019).
[23] M. Pompili, S. L. N. Hermans, S. Baier, H. K. C. Beukers, P. C. Humphreys, R. N. Schouten, R. F. L. Vermeulen, M. J. Tiggelman, L. dos Santos Martins, B. Dirkse, S. Wehner, and R. Hanson, *Realization of a multinode quantum network of remote solid-state qubits*, Science **372**, 259 (2021), https://science.sciencemag.org/content/372/6539/259.full.pdf.
[24] S. Wehner, D. Elkouss, and R. Hanson, *Quantum internet: A vision for the road ahead*, Science **362** (2018), 10.1126/science.aam9288, https://science.sciencemag.org/content/362/6412/eaam9288.full.pdf.
[25] J. I. Cirac, P. Zoller, H. J. Kimble, and H. Mabuchi, *Quantum State Transfer and Entanglement Distribution among Distant Nodes in a Quantum Network*, Phys. Rev. Lett. **78**, 3221 (1997).
[26] H.-J. Briegel, W. Dür, J. I. Cirac, and P. Zoller, *Quantum Repeaters: The Role of Imperfect Local Operations in Quantum Communication*, Phys. Rev. Lett. **81**, 5932 (1998).
[27] N. Sangouard, C. Simon, H. de Riedmatten, and N. Gisin, *Quantum repeaters based on atomic ensembles and linear optics*, Rev. Mod. Phys. **83**, 33 (2011).
[28] G. Chiribella, G. M. D'Ariano, and P. Perinotti, *Theoretical framework for quantum networks*, Phys. Rev. A **80**, 022339 (2009).
[29] C.-Y. Hsieh, *Resource Preservability*, Quantum **4**, 244 (2020).
[30] X. Yuan, Y. Liu, Q. Zhao, B. Regula, J. Thompson, and M. Gu, *Robustness of Quantum Memories: An Operational Resource-Theoretic Approach*, (2019), arXiv:1907.02521 [quant-ph].
[31] S. Langenfeld, O. Morin, M. Körber, and G. Rempe, *A network-ready random-access qubits memory*, npj Quantum Inf. **6**, 86 (2020).
[32] N. Jiang, Y.-F. Pu, W. Chang, C. Li, S. Zhang, and L.-M. Duan, *Experimental realization of 105-qubit random access quantum memory*, npj Quantum Inf. **5**, 28 (2019).
[33] M. Horodecki, P. W. Shor, and M. B. Ruskai, *Entanglement Breaking Channels*, Rev. Math. Phys. **15**, 629 (2003).
[34] M. B. Ruskai, *Qubit Entanglement Breaking Channels*, Rev. Math. Phys. **15**, 643 (2003).
[35] R. Pal and S. Ghosh, *Non-locality breaking qubit channels: the case for CHSH inequality*, J. Phys. A: Math. Theor. **48**, 155302 (2015).
[36] K. Jiráková, A. Černoch, K. Lemr, K. Bartkiewicz, and A. Miranowicz, *Experimental hierarchy and optimal robustness of quantum correlations of two-qubit states with controllable white noise*, (2021), arXiv:2103.03691 [quant-ph].
[37] T. Heinosaari, J. Kiukas, D. Reitzner, and J. Schultz, *Incompatibility breaking quantum channels*, J. Phys. A: Math. Theor. **48**, 435301 (2015).
[38] D. Rosset, F. Buscemi, and Y.-C. Liang, *Resource Theory of Quantum Memories and Their Faithful Verification with Minimal Assumptions*, Phys. Rev. X **8**, 021033 (2018).
[39] M. Piani, *Channel steering*, J. Opt. Soc. Am. B **32**, A1 (2015).
[40] Y.-N. Chen, C.-M. Li, N. Lambert, S.-L. Chen, Y. Ota, G.-Y. Chen, and F. Nori, *Temporal steering inequality*, Phys. Rev. A **89**, 032112 (2014).
[41] T. Fritz, *Quantum correlations in the temporal Clauser–Horne–Shimony–Holt (CHSH) scenario*, New J. Phys. **12**, 083055 (2010).
[42] C. Brukner, S. Taylor, S. Cheung, and V. Vedral, *Quantum Entanglement in Time*, , quant-ph/0402127 (2004), arXiv:quant-ph/0402127 [quant-ph].
[43] J. F. Fitzsimons, J. A. Jones, and V. Vedral, *Quantum correlations which imply causation*, Sci. Rep. **5**, 18281 (2015).
[44] L. Guerini, M. T. Quintino, and L. Aolita, *Distributed sampling, quantum communication witnesses, and measurement incompatibility*, Phys. Rev. A **100**, 042308 (2019), arXiv:1904.08435 [quant-ph].
[45] T. Simnacher, N. Wyderka, C. Spee, X.-D. Yu, and O. Gühne, *Certifying quantum memories with coherence*, Phys. Rev. A **99**, 062319 (2019).
[46] M. F. Pusey, *Verifying the quantumness of a channel with an untrusted device*, J. Opt. Soc. Am. B **32**, A56 (2015).
[47] F. Graffitti, A. Pickston, P. Barrow, M. Proietti, D. Kundys, D. Rosset, M. Ringbauer, and A. Fedrizzi, *Measurement-Device-Independent Verification of Quantum Channels*, Phys. Rev. Lett. **124**, 010503 (2020).
[48] F. Buscemi, *All Entangled Quantum States Are Nonlocal*, Phys. Rev. Lett. **108**, 200401 (2012).
[49] C. Branciard, D. Rosset, Y.-C. Liang, and N. Gisin, *Measurement-Device-Independent Entanglement Witnesses for All Entangled Quantum States*, Phys. Rev. Lett. **110**, 060405 (2013).
[50] Y.-Y. Zhao, H.-Y. Ku, S.-L. Chen, H.-B. Chen, F. Nori, G.-Y. Xiang, C.-F. Li, G.-C. Guo, and Y.-N. Chen, *Experimental demonstration of measurement-device-independent measure of quantum steering*, npj Quantum Inf. **6**, 77 (2020).
[51] Y. Guo, B.-C. Yu, X.-M. Hu, B.-H. Liu, Y.-C. Wu, Y.-F. Huang, C.-F. Li, and G.-C. Guo, *Measurement-device-independent quantification of irreducible high-dimensional entanglement*, npj Quantum Inf. **6**, 52 (2020).
[52] M. T. Quintino, T. Vértesi, D. Cavalcanti, R. Augusiak, M. Demianowicz, A. Acín, and N. Brunner, *Inequivalence of entanglement, steering, and Bell nonlocality for general measurements*, Phys. Rev. A **92**, 032107 (2015).
[53] H.-Y. Ku, S.-L. Chen, N. Lambert, Y.-N. Chen, and F. Nori, *Hierarchy in temporal quantum correlations*, Phys. Rev. A **98**,

022104 (2018).

[54] T. Zhang, O. Dahlsten, and V. Vedral, *Quantum correlations in time*, (2020), arXiv:2002.10448 [quant-ph].

[55] A. J. Leggett and A. Garg, *Quantum mechanics versus macroscopic realism: Is the flux there when nobody looks?*, Phys. Rev. Lett. **54**, 857 (1985).

[56] C. Emary, N. Lambert, and F. Nori, *Leggett-Garg inequalities*, Rep. Prog. Phys. **77**, 016001 (2014).

[57] M. Ringbauer, F. Costa, M. E. Goggin, A. G. White, and A. Fedrizzi, *Multi-time quantum correlations with no spatial analog*, npj Quantum Inf. **4**, 37 (2018).

[58] A. G. Maity, S. Mal, C. Jebarathinam, and A. S. Majumdar, *Self-testing of binary Pauli measurements requiring neither entanglement nor any dimensional restriction*, Phys. Rev. A **103**, 062604 (2021).

[59] J. F. Clauser, M. A. Horne, A. Shimony, and R. A. Holt, *Proposed Experiment to Test Local Hidden-Variable Theories*, Phys. Rev. Lett. **23**, 880 (1969).

[60] R. Augusiak, M. Demianowicz, and A. Acín, *Local hidden-variable models for entangled quantum states*, Journal of Physics A Mathematical General **47**, 424002 (2014), arXiv:1405.7321 [quant-ph].

[61] F. Hirsch, M. T. Quintino, T. Vértesi, M. F. Pusey, and N. Brunner, *Algorithmic Construction of Local Hidden Variable Models for Entangled Quantum States*, Phys. Rev. Lett. **117**, 190402 (2016), arXiv:1512.00262 [quant-ph].

[62] D. Cavalcanti, L. Guerini, R. Rabelo, and P. Skrzypczyk, *General Method for Constructing Local Hidden Variable Models for Entangled Quantum States*, Phys. Rev. Lett. **117**, 190401 (2016), arXiv:1512.00277 [quant-ph].

[63] Y. Zhang, R. A. Bravo, V. O. Lorenz, and E. Chitambar, *Channel activation of CHSH nonlocality*, New J. Phys. **22**, 043003 (2020).

[64] J. Kiukas, C. Budroni, R. Uola, and J.-P. Pellonpää, *Continuous-variable steering and incompatibility via state-channel duality*, Phys. Rev. A **96**, 042331 (2017).

[65] R. Pisarczyk, Z. Zhao, Y. Ouyang, V. Vedral, and J. F. Fitzsimons, *Causal Limit on Quantum Communication*, Phys. Rev. Lett. **123**, 150502 (2019).

[66] J.-D. Lin, W.-Y. Lin, H.-Y. Ku, N. Lambert, Y.-N. Chen, and F. Nori, *Witnessing quantum scrambling with steering*, (2020), arXiv:2003.07043 [quant-ph].

[67] Z. Zhao, R. Pisarczyk, J. Thompson, M. Gu, V. Vedral, and J. F. Fitzsimons, *Geometry of quantum correlations in space-time*, Phys. Rev. A **98**, 052312 (2018).

[68] A. Peres, *Separability Criterion for Density Matrices*, Phys. Rev. Lett. **77**, 1413 (1996).

[69] M. Horodecki, P. Horodecki, and R. Horodecki, *Separability of mixed states: necessary and sufficient conditions*, Physics Letters A **223**, 1 (1996).

[70] S.-L. Chen, N. Lambert, C.-M. Li, A. Miranowicz, Y.-N. Chen, and F. Nori, *Quantifying Non-Markovianity with Temporal Steering*, Phys. Rev. Lett. **116**, 020503 (2016).

[71] J. Kofler and C. Brukner, *Condition for macroscopic realism beyond the Leggett-Garg inequalities*, Phys. Rev. A **87**, 052115 (2013).

[72] R. Uola, G. Vitagliano, and C. Budroni, *Leggett-Garg macrorealism and the quantum nondisturbance conditions*, Phys. Rev. A **100**, 042117 (2019).

[73] H.-Y. Ku, N. Lambert, F.-J. Chan, C. Emary, Y.-N. Chen, and F. Nori, *Experimental test of non-macrorealistic cat states in the cloud*, npj Quantum Inf. **6**, 98 (2020).

[74] D. Maskalaniec and K. Bartkiewicz, *Hierarchy and robustness of multilevel two-time temporal quantum correlations*, (2021), arXiv:2106.02844 [quant-ph].

[75] S. Nagy and T. Vértesi, *EPR Steering inequalities with Communication Assistance*, Sci. Rep. **6** (2016).

[76] H.-Y. Ku, S.-L. Chen, H.-B. Chen, N. Lambert, Y.-N. Chen, and F. Nori, *Temporal steering in four dimensions with applications to coupled qubits and magnetoreception*, Phys. Rev. A **94**, 062126 (2016).

[77] H.-Y. Ku, S.-L. Chen, C. Budroni, A. Miranowicz, Y.-N. Chen, and F. Nori, *Einstein-Podolsky-Rosen steering: Its geometric quantification and witness*, Phys. Rev. A **97**, 022338 (2018).

[78] S.-L. Chen, H.-Y. Ku, W. Zhou, J. Tura, and Y.-N. Chen, *Robust self-testing of steerable quantum assemblages and its applications on device-independent quantum certification*, (2020), arXiv:2002.02823 [quant-ph].

[79] I. Jeon and H. Jeong, *Measurement-device-independent verification of channel steering*, Phys. Rev. A **101**, 012333 (2020).

[80] R. Uola, T. Moroder, and O. Gühne, *Joint Measurability of Generalized Measurements Implies Classicality*, Phys. Rev. Lett. **113**, 160403 (2014).

[81] M. T. Quintino, T. Vértesi, and N. Brunner, *Joint Measurability, Einstein-Podolsky-Rosen Steering, and Bell Nonlocality*, Phys. Rev. Lett. **113**, 160402 (2014).

[82] P. Diviánszky, E. Bene, and T. Vértesi, *Qutrit witness from the Grothendieck constant of order four*, Physical Review A **96** (2017), 10.1103/physreva.96.012113.

[83] M. T. Quintino, J. Bowles, F. Hirsch, and N. Brunner, *Incompatible quantum measurements admitting a local-hidden-variable model*, Physical Review A **93** (2016), 10.1103/physreva.93.052115.

[84] F. Hirsch, M. T. Quintino, and N. Brunner, *Quantum measurement incompatibility does not imply Bell nonlocality*, Phys. Rev. A **97**, 012129 (2018).

[85] J. Fiurášek and Z. Hradil, *Maximum-likelihood estimation of quantum processes*, Phys. Rev. A **63**, 020101 (2001).

[86] Z. Hradil, *Quantum-state estimation*, Phys. Rev. A **55**, R1561 (1997).